

MC Simulations of Self-assembling Hexagonal and Cage-like Bifunctional Periodic Mesoporous Materials

Alessandro Patti^{1,*}, Allan D. Mackie², and Flor R. Siperstein³

¹*Soft Condensed Matter, Debye Institute for NanoMaterials Science, Utrecht University, Princetonplein 5, 3584 CC Utrecht, The Netherlands*

²*Departament d'Enginyeria Química, Universitat Rovira i Virgili, Av. Països Catalans, 26, Tarragona, 43007, Spain*

³*School of Chemical Engineering and Analytical Science, The University of Manchester, PO Box 88, Sacville Street Manchester M60 1QD, UK*

By applying Monte Carlo simulations, we analyze the self-assembly of lyotropic liquid crystalline mesophases in amphiphilic systems. The addition of an inorganic and two hybrid organic-inorganic precursors, one with a bridging and the other with a terminal organic functionality, leads to the formation of bifunctional hexagonally-packed mesoporous materials. These structures exhibit very ordered and uniform mesopores with the organic functional groups located into the cylindrical pores and into their walls, and are found to be stable in a relatively broad range of precursors concentrations. Hexagonal-to-lamellar and hexagonal-to-cubic phase transitions have been observed at constant surfactant concentrations by tuning the relative content of the hybrid precursors which modify the overall solvophilic character of the solvent and, as a consequence, the surfactant solubility in its surrounding environment. The long range ordered cubic phases show interconnected, roughly spherical mesocages of uniform size and interesting distribution of the organic functionalities.

Introduction

Ordered mesoporous materials have attracted the interest of the scientific community since the very beginning of their first synthesis [1, 2]. Their structural properties, such as large surface area and narrow pore size distribution, along with the broad range of possibilities to tune them by changing synthesis conditions, template, and/or (organo)silica precursors, have given an extraordinary impetus to further research aiming to improve their performance in molecular separation, adsorption, catalysis (REF). In particular, much effort has been put on adding functional groups into the pores (REF), into the pore walls [3–5], and, more recently, into both [6, 7]. The incorporation of organosilica precursors (OSPs) of the form $(R'O)_3\text{-Si-R-Si-(OR)'}_3$ into the silica framework, which gave rise to the discovery of periodic mesoporous organosilicas (PMOs) [3–5], can significantly improve the dielectric constant and mechanical properties [27], but, although accessible for reaction, the organic groups in bridging position are not as reactive as those occupying a terminal position in precursors of the form $(R'O)_3\text{-Si-R}$, mainly because of steric and electronic differences [4, 5]. The simultaneous presence of OSPs containing terminal and bridging organic groups leads to bifunctional periodic mesoporous organosilicas (BPMOs) with the functional groups at a nanoscale distance from each other. BPMOs can be obtained by grafting the precursor with a terminal functionality into the pores of PMOs, or in one single step by co-condensation of the two

OSPs, being the most preferred way of synthesis [6–10].

Hexagonally-packed BPMOs were first synthesized by Ozin and coworkers who performed co-condensation of a bridging OSP, bis(triethoxysilyl)ethylene, with a terminal OSP, triethoxyvinylsilane, using cetyltrimethylammonium bromide as structure directing agent [6]. They also proposed the possibility to incorporate a higher number of OSPs, and presented a trifunctional mesoporous structure with one terminal (vynil or methyl) and two bridging (ethylene and methylene) groups. Since then, researchers focused on the incorporation of various OSPs in order to couple different chemical-physical properties together in one single material. Jaroniec et al. used large heterocyclic bridging and mercaptopropyl terminal groups for the adsorption and removal of mercury ions from water solutions [11]; Corriu et al. reported the synthesis of BPMOs with antagonistic bridging acid and terminal basic OSPs for applications as semipermeable membranes [10]; Inagaki et al. obtained sulfuric acid-functionalized mesoporous benzene-silicas to be used as solid acid catalysts [12].

Functionalization of mesoporous materials has been also extended to three-dimensional (3D) cubic mesophases, presenting roughly spherical pores (or cages) interconnected by narrow channels. It is generally accepted that such structures can represent a further improvement with respect to the 1D hexagonally-packed materials, because of their 3D porous network [13, 16]. Their diameter is in the order of 3-9 nm, whereas the linking channels (or windows) show a pretty large range from few angstrom [15] up to several nanometers [16]. In the last fifteen years, self-assembling cage-type mesostructures of different symmetries have been synthesized [17–19] and become more and more attractive

*Electronic address: a.patti@uu.nl

for the possibility to perform a double tuning on the size of the cages and on that of the channels, and, hence, to better control the diffusion of guest molecules in targeted applications [20], such as metal ion trapping [21] or adsorption ([16]). Recently, Garcia-Bennet and coworkers prepared 3D cubic mesocaged materials with $Pm\bar{3}n$ symmetry under strong basic conditions ($pH > 11$) by using a conventional ionic surfactant, cetyltriethylammonium bromide (CTEABr), and two common silica precursors, tetraethyl orthosilicate (TEOS) and (3-aminopropyl)triethoxysilane (APES) [22]. They performed several one-pot syntheses at different molar ratios surfactant/APES and found a cubic structure when this ratio is 0.6. The main effect of APES in the mechanism proposed by these authors is based on the penetration of its solvophobic chain into the aggregates, rather than in the interactions that could be established between the charged ammonium ions and the surfactant headgroups, which, instead, explains the formation of mesocages of face-centered cubic symmetry [23]. Among other functional groups, amines are of great interest for CO₂ capture and separation and for removal of heavy ions from water solutions. Kao *et al.* obtained under acid conditions very ordered and stable amino-functionalized cubic SBA-1 mesoporous materials by co-condensation of TEOS with (3-aminopropyl)trimethoxysilane using CTEABr as template [24].

To the best of our knowledge, the first attempt to synthesize bifunctional cage-like mesoporous materials is very recent and due to Wu *et al.* [25]. By one-pot synthesis, the authors prepared functionalized SBA-1 mesophases [17] containing ethane bridging groups in the silica framework and terminal thiol groups in the pore channels, by using CTEABr as template. The resulting material revealed good adsorption properties for mercury ions and, hence, a potential role in soil and water remediation. Jaroniec and coworkers obtained mesoporous organosilicas by co-condensation of TEOS with two organosilica precursors containing bridging isocyanurate and ethane groups [13]. Their main aim was to test a method for the template removal based on a short extraction and a soft heating under nitrogen. The characterization of the resulting material by different techniques showed that, although a significant shrinkage was detected, the order of the structure was preserved.

In this work, we performed Monte Carlo (MC) simulations to model the self-assembly of BPMOs obtained by co-condensation of two hybrid OSPs and a pure silica precursor. Our interest is mainly focused on the analysis of the hexagonally-packed and cage-like cubic structures and, in particular, on the distribution of the functional groups in their pores and pore walls. On the other hand, we analyze the transition from hexagonal to cubic cage-like phases which is deeply linked to the concentration of the hybrid organosilica precursors in the system.

Model and Simulation Methodology

We studied the self-assembly of liquid crystalline mesophases by using a coarse-grained lattice model, first applied by Larson and coworkers who investigated the aggregation behavior of amphiphilic monomers in systems containing water-like and oil-like solvents [26]. In this model, space is organized into a three dimensional cubic network of sites, which are all occupied by the solvent, precursors, or surfactant. As already explained in previous works [28, 29], the advantage of this model is that it permits to better appreciate the ordered periodicity of the mesoporous structures obtained, by reducing the many complex properties of the system to the most representative ones. Our system is composed of five components being modelled as chains of connected sites (see Figure 1): a surfactant, T₅HH₃, with a linear solvophobic tail of five segments T , and a solvophilic bulky head made up of four segments H ; a pure silica precursor, I₂; two OSPs, I₂THT₃ and I₂THTI₂, with a terminal and a bridging organic functionality, respectively; and a solvent, S , which has not been modelled explicitly. Each segment occupies one single site of the lattice box, and hence no overlaps are allowed. From now on, we call the tail beads in bridging position between H and I , T_α , regardless of the precursor they belong to.

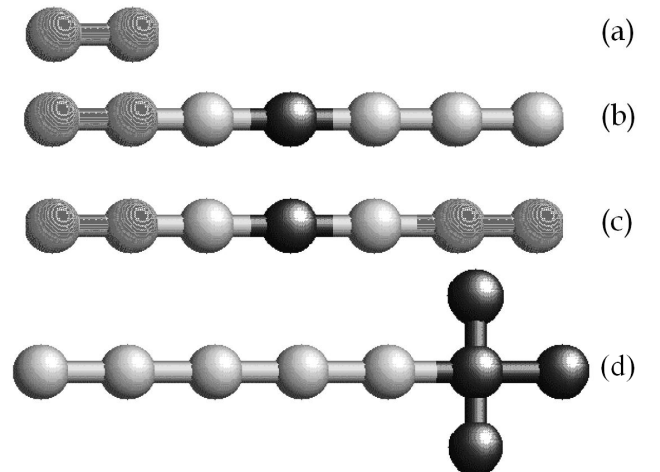


FIG. 1: Modelled precursor and surfactant chains. (a) Pure silica precursor, I₂; (b) OSP I₂THT₃; (c) OSP I₂THTI₂; (d) surfactant T₅HH₃.

The T (H) segments belonging to the precursors are as solvophobic (solvophilic) as the ones of the surfactant chains, whereas the inorganic bead, I , has a strong interaction with the surfactant heads and is soluble in the solvent. Each bead interacts with its nearest and diagonally-nearest neighbors, which define the coordination number of the cubic lattice, that is $z = 26$. The global interchange energy between a generic pair of sites i and j is defined as

$$\omega_{ij} = \epsilon_{ij} - \frac{1}{2}(\epsilon_{ii} + \epsilon_{jj}) \quad (1)$$

with $i \neq j$ and ϵ_{ij} the individual pair interactions. A detailed summary of the all bead-bead interactions is given in Table I.

TABLE I: Individual and global interchange energies between the beads in the system.

Pair of beads	H-H	H-T	H-I	H-S	T-T	T-I	T-S	I-I	I-S	S-S
ϵ_{ij}	0	0	-2	0	-2	0	0	0	0	0
ω_{ij}	0	1	-2	0	0	1	1	0	0	0

In order to displace the chains in the simulation box and hence make the system evolve from a completely random configuration to an ordered configuration, we performed Monte Carlo simulations in the NVT ensemble. An elongated box of volume $24 \times 24 \times 100$ was used to study the phase separation between a hybrid-rich phase and a solvent-rich phase; whereas a cubic box of volume 40^3 was used to analyze the structural properties of the resulting ordered mesophases. In both cases, periodic boundary conditions were applied. All the chains have been displaced by configurational bias moves (partial and complete regrowth) [30]. The linear precursor chains were also moved by reptation, according to the Metropolis algorithm. The dimensionless temperature reads $T^* = k_B T / \omega_{HT}$, where k_B is the Boltzmann constant, T the absolute temperature, and ω_{HT} is the surfactant head-tail interaction energy. All the simulations have been run at $T^* = 8.0$.

To check the distribution of the hybrid precursors into the silica framework, we calculated the composition profiles $\rho_i(r)$ of the sites i at radial distance r from the center of mass in spherical aggregates, or from the line connecting the center of mass of quasi-circular cross-sections in cylindrical aggregates. We assume that two surfactant chains belong to the same aggregate if they share at least one of their tail beads as a neighbor (see [28] for more details). Since the volume fraction of the precursors can be much smaller than that of the surfactant, we prefer to normalize the density profiles by dividing $\rho_i(r)$ by the global density $\rho_{i,0}$. $\rho_{i,N}(r) \equiv \rho_i(r) / \rho_{i,0}$ should converge to 1 at large radial distances r .

Results

Since no phase diagrams are available for such model system, we referred to the phase behavior of the four-components system, $T_5HH_3/I_2/I_2THT_3/S$, discussed in a previous work [31], to locate the region of existence of ordered mesophases, and gradually increased the concentration of the new added OSP, I_2THTI_2 . Generally,

we observed the formation of hexagonally-packed liquid crystals as a result of the phase separation between a surfactant-rich phase and a solvent-rich phase, as shown in Figure 2.

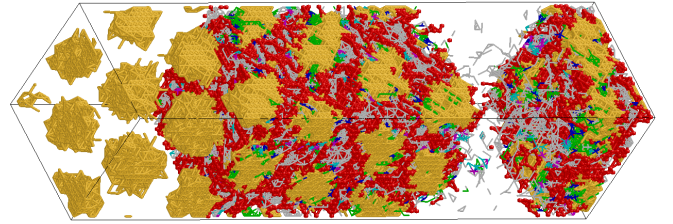


FIG. 2: Hexagonally-packed phase at equilibrium with a solvent-rich phase observed at $T^* = 8.0$ in a lattice box of volume $24 \times 24 \times 100$. Global concentrations: 40% T_5HH_3 - 10% I_2 - 10% I_2THT_3 - 4% I_2THTI_2 . Surfactant heads and tails are shown in red and yellow, respectively; the inorganic beads in gray; H beads of I_2THT_3 in blue; H beads of I_2THTI_2 in magenta; T beads of I_2THT_3 in green; T beads of I_2THTI_2 in cyan. The solvent is not shown. Only the surfactant tails are shown in the left side of the box to appreciate the hexagonal order. Color online.

The phase separation takes origin from (i) the strong attraction between the inorganic beads of the precursors and the surfactant heads and (ii) the repulsion between the surfactant tails with the solvent and with the surfactant heads (see Table I).

Previously, we had shown that in systems containing high concentrations of I_2THT_3 and no I_2THTI_2 , a transition from hexagonal to lamellar phases was detected [31]. This result, observed experimentally in systems containing the hybrid precursor phenyl-3-aminopropyltrimethoxysilane [32], was imputed to the strong solvophobic character of I_2THT_3 which swells the core of the cylindrical aggregates and leads to the formation of lamellar structures. If we add I_2THTI_2 to the system, it self-assembles in hexagonally ordered structures in a broad range of concentrations, unless the ratio between the volume fractions of the two OSPs becomes $\phi \gg 1$ or $\phi \ll 1$ (see Table II). In these extreme cases, the distinctive nature of the two OSPs emerges and affects the order of the phases at equilibrium. In particular, by further increasing the concentration of the bridging OSP and decreasing that of the terminal OSP, we notice a gradual transition to a cubic phase. Viceversa, if the concentration of the bridging precursor goes gradually to zero, we first detect a two-phase region of lamellar-hexagonal coexistence and, when the bridging precursor is completely removed, a stable lamellar phase. Exemplarily, in Figure 3 we give two equilibrium configurations of a hexagonal-lamellar coexistence (a) and a 3D cubic mesophase (b). In both cases, some of the aggregates are

shown only with their solvophobic core to better appreciate the structural order.

TABLE II: Global concentrations of I_2THT_3 and I_2THTI_2 in systems containing 40% T_5HH_3 and 10% I_2 . H : hexagonal, C : cubic, L : lamellar, L/H : hexagonal-lamellar coexistence.

I_2THT_3 (%)	I_2THTI_2 (%)	Order
0.0 - 5.0	0.0 - 15.0	H
0.0	30.0	C
5.0	20.0 - 30.0	C
10.0 - 15.0	0.0 - 20.0	H
18.0 - 25.0	0.0	L
20.0	2.0	L/H
20.0	5.0 - 15.0	H
30.0	2.0 - 5.0	L/H

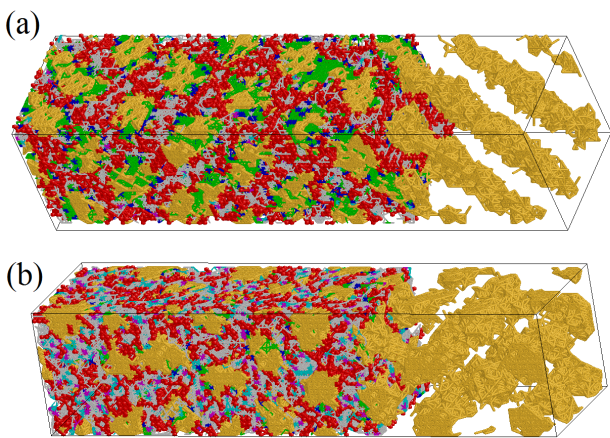


FIG. 3: (a) Hexagonal-lamellar coexistence observed in the system 40% T_5HH_3 , 10% I_2 , 2% I_2THTI_2 , 30% I_2THT_3 and 18% solvent. (b) Cage-like cubic structure obtained in the system 40% T_5HH_3 , 10% I_2 , 20% I_2THTI_2 , 5% I_2THT_3 and 25% solvent. The solvent is not shown. In the right side of the boxes, only the surfactant tails are shown to appreciate the lamellar (a) and cubic (b) structural order. See caption of Figure 2 for colors. Color online.

The hexagonal-to-cubic and hexagonal-to-lamellar phase transitions are the result of the increasing concentration of I_2THTI_2 and I_2THT_3 , respectively. Due to the presence of a double inorganic terminal group, $-I_2$, forming a very strong attraction with the surfactant heads, the precursor I_2THTI_2 behaves like a cosolvent and improves the solubility of the surfactant in the system. On the other hand, the strong solvophobic terminal group in I_2THT_3 behaves like a cosurfactant and increases the overall solvophobic nature of the solvent.

In figures 4 and 5, the normalized density profiles of the organic functional groups of I_2THT_3 and I_2THTI_2 , respectively, are given. In order to locate their position

with respect to the inorganic framework, the distribution of the inorganic beads, I , of the pure silica and OSPs, is added in both figures. The total amount of I beads constitutes the silica framework surrounding the aggregates, and therefore it is important to individuate the location of the functional groups with respect to it. Each of the three distribution profiles of the organic beads belonging to I_2THT_3 reveals very well defined peaks, being clearly separated from that of the inorganic moiety surrounding the pore. This is especially evident for the terminal solvophobic group, $-T_3$, being almost completely accumulated inside the mesopores and absent in the pore walls, in agreement with experimental results (REF). A similar result was formerly obtained in systems containing only one hybrid precursor, I_2THT_3 , [31], and, hence, the high concentration of the terminal functionality in the solvophobic core does not seem to be affected by the presence of a second hybrid precursor.

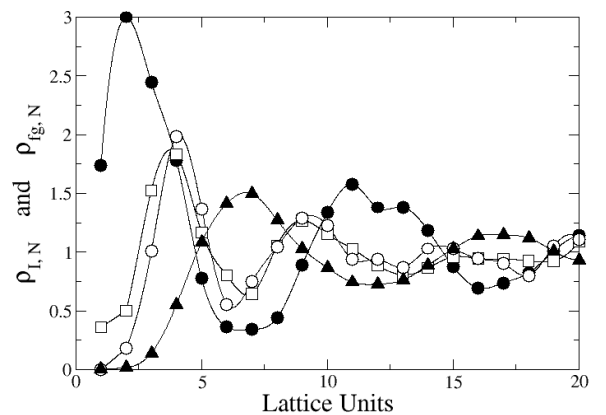


FIG. 4: Normalized distribution profiles of the functional group of I_2THT_3 in systems containing 51.8% T_5HH_3 , 11.8% I_2 , 5.1% I_2THT_3 and 12.1% I_2THTI_2 . Symbols: T_α (\square), $T_{terminal}$ (\bullet), H (\circ). The symbols (\blacktriangle) refer to the overall normalized distribution of the inorganic moiety, I , belonging to all precursors.

On the other hand, Figure 5 brings to light a very deep interconnection between the organic bridging functional group of I_2THTI_2 and the inorganic framework, as confirmed by the quasi-overlap of the corresponding density profiles. The split detected in the peak of the T_α profile arises from the intrinsic symmetric architecture of the bridging precursor, and creates a sort of protecting covering around the solvophilic functional bead H . This covering could represent a critical barrier in case the solvophilic functional group had to play a role as active site for a given application.

The cubic phase is characterized by the presence of (roughly) spherical aggregates whose size distribution, giving the probability to observe a cluster of a given size

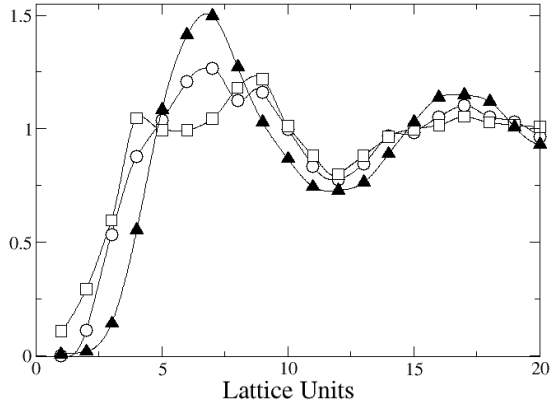


FIG. 5: Normalized distribution profiles of beads belonging to I_2THTI_2 in systems containing 51.8% T_5HH_3 , 11.8% I_2 , 5.1% I_2THT_3 and 12.1% I_2THTI_2 . Symbols: T_α (\square), H (\circ). The symbols (\blacktriangle) refer to the overall normalized distribution of the inorganic moiety, I , belonging to all precursors.

along a simulation run, is relatively narrow and peaked at approximately 60 chains, as showed in Figure 6. The smaller peaks, being located at $N \approx 120, 180,$ and $240,$ do not indicate the presence of elongated micelles, but rather the probability of two, three, or four solvophobic cores to touch each other. Due to the high density in our system, this transitory event can be easily detected, especially for pairs of aggregates (see Figure 7 (b)), but also for triplets or quadruplets. In the inset of Figure 6, we give the radii of gyration R_g of the clusters, whose value, which is slightly less than 3, is practically constant for all the clusters observed in the system.

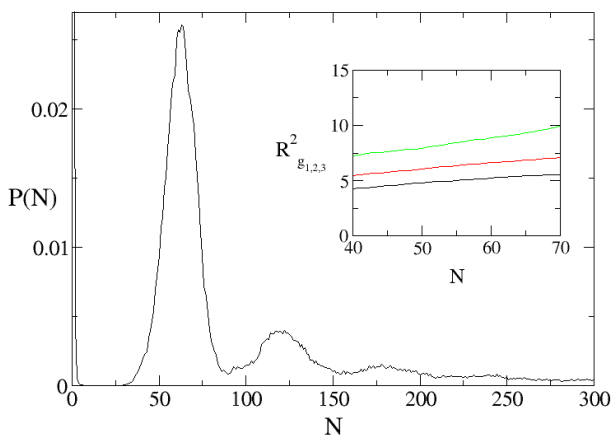


FIG. 6: Cluster size distribution and (inset) principal radii of gyration of a system containing 40% T_5HH_3 , 10% I_2 , 20% I_2THTI_2 , 5% I_2THT_3 and 25% solvent.

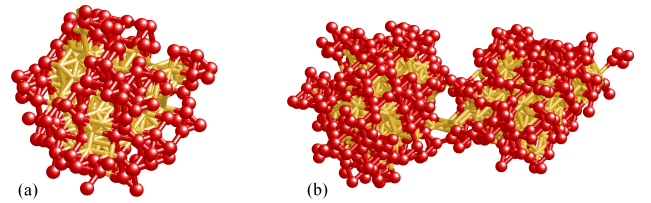


FIG. 7: (a, b) Spherical aggregates observed in a system containing 40% T_5HH_3 , 10% I_2 , 30% I_2THTI_2 , and 20% solvent. No OSP with terminal organic group is present. In (b) two aggregates are touching each other. The tails and heads are in yellow and red, respectively. Color online.

A clear representation of the cage-to-cage interconnection is shown in Figure 8, where three spherical aggregates have been isolated from their bulk phase. The section (c) of the interconnected aggregates displays the formation of two crossing quasi-cylindrical pores with periodic *bottlenecks* whose diameter depends on the distance between the cages, that is on the surfactant concentration, but, more generally, also on the architecture of the surfactant head. At low surfactant concentrations, the aggregates would be completely separated by the inorganic wall and no interconnecting channels would be observed. However, a long linear headgroup could balance this effect. If we look at the density distribution profiles of Figure 9, we see that the most of the inorganic layer is located around the corona of the aggregates, where the concentration of the surfactant heads show a peak as well. From this figure, we observe that the pure silica and hybrid precursors do not exhibit a density peak separating the coronas of neighboring aggregates, but, instead, they organize around them, and, once the template has been removed, form interconnecting channels. As also observed for hexagonally-packed phases, the terminal solvophobic group of I_2THT_3 penetrates deeply inside the core of the cage, whereas the other functional groups are most likely distributed around or into the solvophilic corona. For cubic mesophases not containing terminal OSP, the density distribution of the surfactant and precursors do not show significant differences from those in Figure 9, and are not shown here.

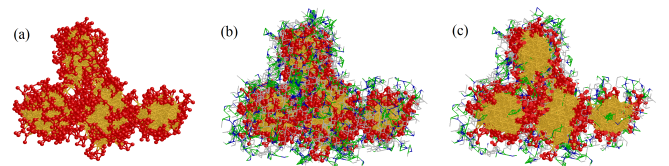


FIG. 8: Snapshot of four interconnected mesocages observed in the system containing 40% T_5HH_3 , 10% I_2 , 20% I_2THTI_2 , 5% I_2THT_3 and 15% solvent. (a) Template only: surfactant heads and tails are in red and yellow, respectively. (b) Cages covering the template: I , H , and T beads of the precursors are in grey, blue, and green, respectively. (c) Section. Color online.

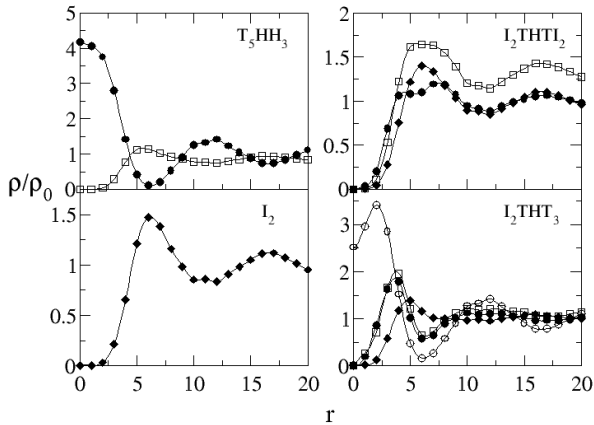


FIG. 9: Normalized density profiles observed in a spherical aggregate with 60 surfactant chains. The squares, diamonds, solid and empty circles represent H , T , I , and $T_{terminal}$ beads, respectively. Concentrations: 40% T_5HH_3 , 10% I_2 , 20% I_2THTI_2 , 5% I_2THT_3 and 15% solvent.

Conclusions

We performed computer simulations to study the phase behavior and the self-assembly of systems composed by an amphiphilic template, a pure silica precursor, two organosilica precursors with terminal or bridging functionalities, and a solvent. By using a simple coarse-grained model, we showed that these systems are able to form bifunctional ordered mesophases, such as lamellar, cage-like cubic, or hexagonally-packed cylindrical structures. By tuning the concentrations of the two hybrid organosilica precursors, which have opposite effects on the solubility of the surfactant, hexagonal-to-lamellar or hexagonal-to-cubic phase transitions are observed. In particular, by increasing the concentration of the bridging precursor, which behaves as a cosolvent, we favour the formation of the cubic phase, whereas a high concentration of the terminal precursor, which can be considered as a cosurfactant, leads the system to form lamellar phases. Removing the template from the hexagonally-packed or cubic phases leads to the formation of mesoporous structures containing functional organic groups in the silica framework and in the pores. The distribution of these groups has been discussed in terms of composition profiles, and displayed the possibility to use them as active sites for selective operations. The transition from hexagonal to cubic phases gives rise to the formation of interconnected spherical cavities (or cages). Networks of 3D quasi-cylindrical pores with periodical bottlenecks located at the intersection of neighboring cages have been observed and the composition profiles of the functional groups into the pores and into the pore walls, result to

be basically identical to those observed for the cylindrical aggregates.

- [1] J. S. Beck, J. C. Vartuli, W. J. Roth, M. E. Leonowicz, C. T. Kresge, K. D. Schmitt, C. T. W. Chu, D. H. Olson, E. W. Sheppard, S. B. Mccullen, J. B. Higgins, and J. L. Schlenker, *Journal of the American Chemical Society* 114 (1992) 10834.
- [2] C. T. Kresge, M. E. Leonowicz, W. J. Roth, J. C. Vartuli, and J. S. Beck, *Nature* 359 (1992) 710.
- [3] T. Asefa, M. J. MacLachan, N. Coombs, and G. A. Ozin, *Nature* 402 (1999) 867.
- [4] S. Inagaki, S. Guan, Y. Fukushima, T. Ohsuna, and O. Terasaki, *Journal of the American Chemical Society* 121 (1999) 9611.
- [5] B. J. Melde, B. T. Holland, C. F. Blanford, and A. Stein, *Chemistry of Materials* 11 (1999) 3302.
- [6] T. Asefa, M. Kruk, M. J. MacLachlan, N. Coombs, H. Grondey, M. Jaroniec, and G. A. Ozin, *J. Am. Chem. Soc.* 123 (2001) 8520.
- [7] E. Besson, A. Mehdi, V. Matsura, Y. Guari, C. Reye, and R. J. P. Corriu, *Chemical Communications* (2005) 1775.
- [8] M. C. Burleigh, M. A. Markowitz, M. S. Spector, and B. P. Gaber, *Chem. Mater.* 13 (2001) 4760.
- [9] M. C. Burleigh, M. A. Markowitz, M. S. Spector, and B. P. Gaber, *J. Phys. Chem. B* 105 (2001) 9935.
- [10] J. Alauzun, A. Mehdi, C. Reye, and R. J. P. Corriu, *J. Am. Chem. Soc.* 128 (2006) 8718.
- [11] O. Olkhoviyk, S. Pikus, and M. Jaroniec, *J. Mater. Chem.* 15 (2005) 1517.
- [12] Q. H. Yang, M. P. Kapoor, and S. Inagaki, *J. Am. Chem. Soc.* 124 (2002) 9694.
- [13] R. M. Grudzien, J. P. Blitz, S. Pikus, M. Jaroniec, *Micropor. and Mesopor. Mater.* 118 (2009) 68.
- [14] S. Kamiya, H. Tanaka, S. Che, T. Tatsumi, O. Terasaki, *Solid State Sci.* 5 (2003) 197.
- [15] T.-W. Kim, R. Ryoo, M. Kruk, K. P. Gierszal, M. Jaroniec, S. Kamiya, O. Terasaki, *J. Phys. Chem. B* 108 (2004), 11480.
- [16] J. Fan, C. Yu, F. Gao, J. Lei, B. Tian, L. Wang, Q. Luo, B. Tu, W. Zhou, D. Zhao, *Angew. Chem., Int. Ed.* 42, (2003) 3146.
- [17] Q. Huo, D. I. Margolese, U. Ciesla, P. Feng, T. E. Gier, P. Sieger, R. Leon, P. M. Petroff, F. Schth, and G. D. Stucky, *Nature* 368 (1994) 317.
- [18] C. Yu, Y. Yua, and D. Zhao, *Chem. Commun.* (2000) 575.
- [19] A. E. Garcia-Bennett, K. Miyasaka, O. Terasaki, and S. N. Che, *Chem. Mater.* 16 (2004) 3597.
- [20] Q. S. Huo, D. I. Margolese, U. Ciesla, P. Y. Feng, T. E. Gier, P. Sieger, R. Leon, P. M. Petroff, F. Schuth, and G. D. Stucky, *Nature* 368 (1994) 317. A. E. Garcia-Bennett, K. Miyasaka, O. Terasaki, S. N. Che, *Chem. Mater.* 16 (2004), 3597. C. Zapilko, Y. Liang, and R. Anwender, *Chem. Mater.* 19 (2007), 3171.
- [21] S. A. El-Safty, A. A. Ismail, H. Matsunaga, H. Nanjo, and F. Mizukami, *J. Phys. Chem. C* 112 (2008) 4825.
- [22] R. Atluri, Y. Sakamoto, and A. E. Garcia-Bennett, *Langmuir* 25 (2009) 3189.

- [23] S. N. Che, A. E. Garcia-Bennett, T. Yokoi, K. Sakamoto, H. Kunieda, O. Terasaki, and T. Tatsumi, *Nat. Mater.* 2 (2003) 801.
- [24] H. Kao, C. Liao, A. Palani, Y. Liao, *Micropor. and Mesopor. Mater.* 113 (2008) 212.
- [25] H. Wu, C. Liao, Y. Pan, C. Yeh, H. Kao, *Micropor. and Mesopor. Mater.* 119 (2008) 109.
- [26] R. G. Larson, L. E. Scriven, and H. T. Davis, *J. Chem. Phys.* 83 (1985) 2411.
- [27] Y. F. Lu, H. Y. Fan, N. Doke, D. A. Loy, R. A. Assink, D. A. LaVan, and C. J. Brinker, *J. Am. Chem. Soc.* 122 (2000) 5258.
- [28] A. Patti, A. D. Mackie, and F. R. Siperstein, *Langmuir* 23 (2007) 6771.
- [29] A. Patti, F. R. Siperstein, and A. D. Mackie, *J. Phys. Chem. C* 111 (2007) 16035.
- [30] D. Frenkel and B. Smit, *Understanding Molecular Simulations: From Algorithms to Applications*, Academic Press, San Diego, 2001.
- [31] A. Patti, A. D. Mackie, V. Zelenak, and F. R. Siperstein, *J. Mater. Chem.* 19, (2009) 724.
- [32] V. Zelenak, M. Badanicova, N. Murafa, and U. Vannio, unpublished work